

Self-Organized Criticality with Complex Scaling Exponents in the Train Model

Franz-Josef Elmer

Institut für Physik, Universität Basel, CH-4056 Basel, Switzerland

(September, 1997)

The train model which is a variant of the Burridge-Knopoff earthquake model is investigated for a velocity-strengthening friction law. It shows self-organized criticality with complex scaling exponents. That is, the probability density function of the avalanche strength is a power law times a log-periodic function. Exact results (scaling exponent: $3/2 + 2\pi i / \ln 4$) are found for a nonlocal cellular automaton which approximates the overdamped train model. Further the influence of random static friction is discussed.

PACS numbers: 64.60.Lx, 05.70.Ln

Ten years ago Bak, Tang, and Wiesenfeld showed that a weakly driven dissipative system with many metastable states can organize itself into a critical state in the sense of a second-order phase transition [1]. Because criticality is characterized by scale invariance they expect power-law behavior. For example the probability density function of the strength S of the restructuring events (avalanches) should scale like $1/S^B$ where B is some positive real number.

In continuous scale invariance the scaling factor λ can be arbitrary. This invariance is partially broken if λ is restricted to a specific value $\tilde{\lambda}$ and its integer powers $\tilde{\lambda}^n$. This *discrete scale invariance* has a profound consequence [2]. It leads to *complex* scaling exponents $B + iC$, where $C = 2\pi / \ln \tilde{\lambda}$. More precisely: The scaling function has the form $S^{-B} f(C \ln S)$, where f is a 2π -periodic function. Sornette and collaborators have shown that such scaling functions are common in many areas, e.g. fractals, deterministic chaos, dendritic growth and rupture [2].

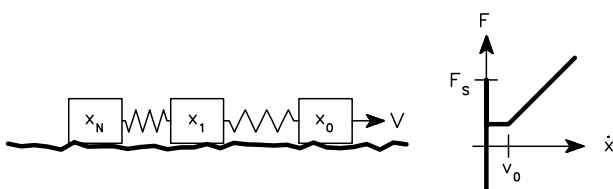


FIG. 1. The train model and the phenomenological friction law (2).

In this paper we present two models which exhibit self-organized criticality (SOC) with complex scaling exponents. The first model is the train model [3] which is a variant of the well-known Burridge-Knopoff (BK) earthquake model [4]. In the literature the BK model and the train model are treated as examples of weakly driven dis-

sipative systems with many metastable states. In both models power laws for the avalanche (earthquake) statistics have been found. In most of these studies an unrealistic purely velocity-weakening friction law is used. But any phenomenological friction law has to be velocity-strengthening for large velocities. Here we use a *realistic* friction law (see Fig. 1) which is a velocity independent Coulomb law for small velocities. For velocities larger than v_0 it is proportional to the velocity [5]. Our second model is a nonlocal cellular automaton which approximates the train model in the overdamped limit.

The train model is a finite chain of $N + 1$ blocks on a rough surface. The blocks are coupled by springs and the interaction with the surface is described by a phenomenological dry-friction law F (see Fig. 1):

$$M\ddot{x}_j + F(\dot{x}_j) = \kappa(x_{j+1} - 2x_j + x_{j-1}), \quad j = 1, \dots, N, \quad (1)$$

where M is the mass of a block, x_j is the position of block j , and κ is the stiffness of the springs. The system is driven by pulling block zero with a very small velocity v , i.e., $x_0 = vt$. The other end of the chain is free, i.e., $x_{N+1} = x_N$. Our friction law F reads:

$$F(\dot{x}) = \begin{cases} (-\infty, F_S] & \text{if } \dot{x} = 0; \\ \gamma v_0 & \text{if } 0 < \dot{x} < v_0; \\ \gamma \dot{x} & \text{if } \dot{x} > v_0. \end{cases} \quad (2)$$

A resting block starts sliding if the sum of the spring forces is larger than F_S . The friction law does not allow backward motions because the static friction can take any negative value. The kinetic friction force is a monotonically increasing function of the velocity. We assume $\gamma v_0 < F_S$ otherwise the chain would not show avalanches. In the simulation we drive the system infinitesimally slowly. This can be achieved in the following way. During an avalanche x_0 is held constant. After the avalanche, when all blocks are at rest (i.e., $\dot{x}_j = 0$), we set $x_0 = (1 + \epsilon)F_S/\kappa - x_2 + 2x_1$, with $\epsilon \ll 1$. Thus the force on block number one is $(1 + \epsilon)F_S$ and just exceeds the threshold for sliding. Usually we have chosen $\epsilon = 10^{-4}$.

Figure 2 shows the evolution of the model for two different values of the damping constant γ . The avalanches always start at the pulling end. They propagate up to a certain block. This is the reason for the tree-like structures seen in Fig. 2. We characterize the avalanches by two quantities which have a simple geometric meaning in Fig. 2: The length L and the strength S defined by

$$S = \sum_{j=1}^N |x_j^{\text{after}} - x_j^{\text{before}}|, \quad (3)$$

where x_j^{before} and x_j^{after} are the position of the block j before and after the avalanche. The length L is the number of blocks that are involved in the avalanche, i.e., $x_j^{\text{after}} \neq x_j^{\text{before}}$. For non-system-spanning avalanches (i.e., $L < N$) this quantity corresponds to the height of the branching points in the tree. In Fig. 2 the area below a branching point is just S .

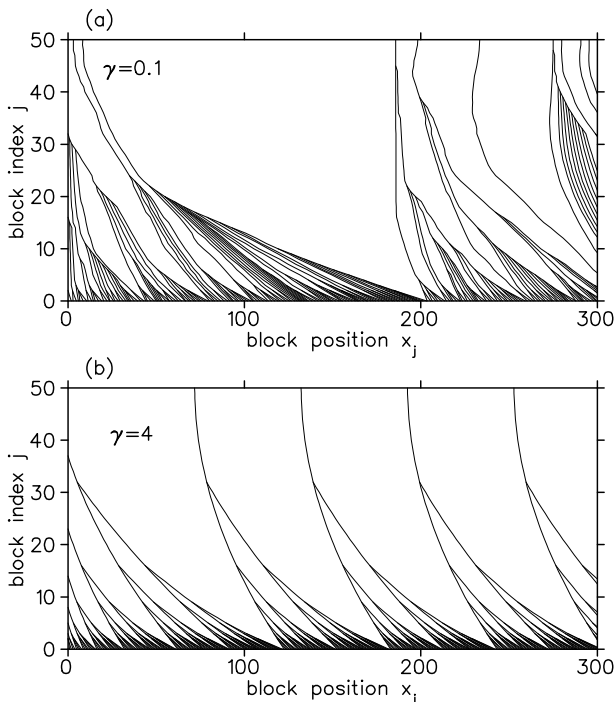


FIG. 2. The positions of the blocks just before an avalanche starts. Several hundreds of avalanches are shown. The parameters are $N = 50$, $v_0 = 0.01$, $M = F_S = \kappa = 1$. The initial values are $x_j(0) = 0$, for $j = 0, \dots, N$.

We see a clear distinctive behavior between the underdamped case ($\gamma = 0.1$) and the overdamped case ($\gamma = 4$) [6]. The underdamped case is characterized by chaotic motion of the chain leading to an irregular sequence of avalanches even for nonrandom initial conditions [3]. In the overdamped case the motion is very regular. After the transient which is finished after the first system-spanning avalanche the same sequence of avalanches reappears periodically. In both cases SOC with discrete scale invariance occurs. But the details are different.

First we investigate the underdamped case. Fig. 3 shows the cumulative density $P(S)$ for five different values of the system length N . The cumulative density $P(S)$ is the probability to find an avalanche that is stronger than S . The cumulative densities for S show steps for large avalanches. Let us assume that $P(S)$ fulfill a usual

finite-size scaling ansatz, i.e.,

$$P(S) = S^{-\sigma} G(S/N^\alpha). \quad (4)$$

Note that $B = \sigma + 1$ because the probability density function is the derivative of P . The inset of Fig. 3 shows the best approach to such an ansatz. The value of α was obtained from a fit of the averaged values of S for the system-spanning avalanches which are responsible for the last step in the cumulative density. This fit yields $\alpha = 2.34 \pm 0.02$. For the value of σ we have chosen $\sigma = 1 - 1/\alpha$ because a sum rule $\langle S \rangle \sim N$ has to be fulfilled [3].

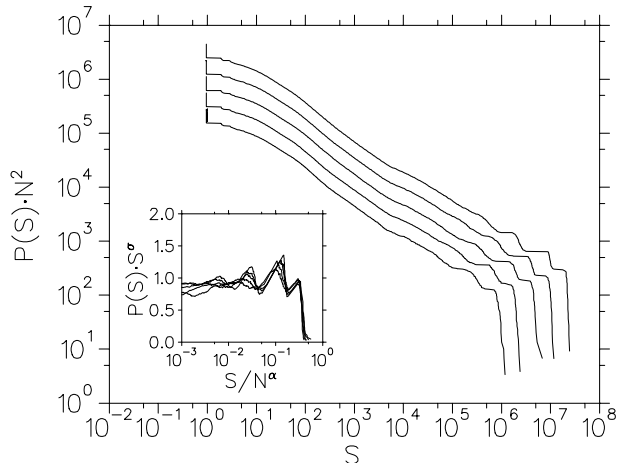


FIG. 3. The cumulative density $P(S)$. The parameters are $\gamma = 0.1$, $v_0 = 0.01$, $M = F_S = \kappa = 1$, and $N = 530, 750, 1060, 1500$, and 2121 . The curves are shifted by $2 \log N$ in order to separate them. The inset shows the results of finite-size scaling with $\alpha = 2.34$ and $\sigma = 1 - 1/\alpha = 0.573$.

Although the finite-size scaling ansatz is not completely satisfactory, one has the impression that for increasing N the scaling functions are approaching a sawtooth function. In other words, the cumulative density has steps which becomes steeper and steeper for increasing N and larger S . The scaling function shows oscillations which are periodic in the logarithm of the argument. This is a clear sign of discrete scale invariance. The numerically obtained scaling factor is $\tilde{\lambda} = 4.3 \pm 0.4$. Thus the complex exponent of the probability density function reads $B + iC = \sigma + 1 + 2\pi i / \ln \tilde{\lambda} \approx 1.573 + 4.3i$.

The selfsimilarity of the avalanche tree in Fig. 2(b) reflects the discrete scale invariance in the overdamped case. Between two system-spanning avalanches, $2^n - 1$ avalanches occur. Here $n = 1 + \text{int}(\log N / \log 2)$, where $\text{int}(x)$ denotes the largest integer smaller than x . There are only n different avalanche lengths and sizes. The m -th type of avalanche occurs 2^{n-m} times. Its length is $L = 2^{m-1}$. Thus, the scaling factor is two. The cumulative density $P(L)$ is in a log-log plot a staircase with stairs of equal heights and widths [7]. A similar staircase is found for $P(S)$. Here the scaling factor is $\tilde{\lambda} = 2^2 = 4$ because S

corresponds to an area in Fig. 2. The critical exponents are $\alpha = 2$ and $\sigma = 0.5$. Thus $B + iC = 3/2 + 2\pi i / \ln 4$.

The overdamped behavior of the train model can be mimicked by the following *nonlocal* cellular automaton. The state of each cell is given by the block positions x_j and a boolean variable s_j which is *true* when the block slides, otherwise it is *false*. The driving rule is the same as in the train model, i.e., $x_0 = (1 + \epsilon)F_S/\kappa - x_2 + 2x_1$.

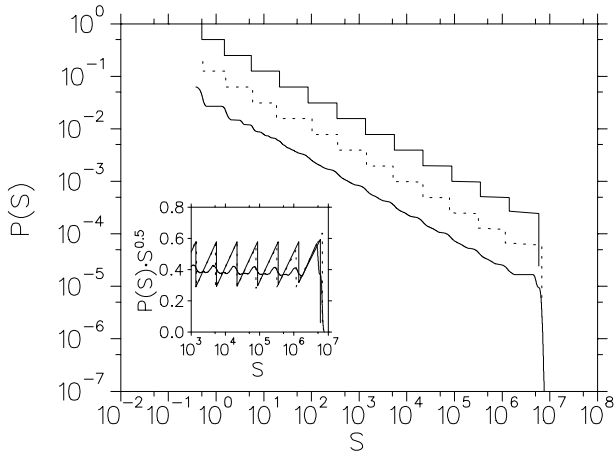


FIG. 4. The cumulative density $P(S)$ for the deterministic cellular automaton for the overdamped train model with and without randomly chosen constant static forces F_S . The parameters are $\langle F_S \rangle = \kappa = 1$ and $N = 2121$. The curves are shifted in order to distinguish them. The upper solid curve is the nonrandom case, i.e. $\Delta F_S = 0$. The middle dashed curve is one realization of the random static friction taken from a Gaussian distribution with $\Delta F_S = 0.1$. The lower solid curve is an average over 1000 realizations of the random static friction. The inset shows the scaling functions.

The relaxation rules are the following: (i) First the forces $f_j \equiv \kappa(x_{j-1} - 2x_j + x_{j+1}) - F_S$ are calculated. The variable s_j is *true* if and only if $f_j > 0$. (ii) In the second step the positions of all sliding blocks are updated simultaneously in the following way:

$$x_j = x_{j_1} + \frac{x_{j_2} - x_{j_1}}{j_2 - j_1}(j - j_1), \quad \text{for } j_1 < j < j_2, \quad (5)$$

where j_1 and j_2 are the left-nearest and right-nearest non-sliding blocks. That is, $s_{j_1} = s_{j_2} = \text{false}$ and $s_j = \text{true}$, for $j_1 < j < j_2$. The consequence of this rule is that $x_{j-1} + x_{j+1} - 2x_j = 0$, for $j_1 < j < j_2$. Note that $s_0 \equiv s_{N+1} \equiv \text{false}$. If $j_2 = N + 1$ then $x_{j_2} = x_{j_1}$ in (5). This rule gives the result of a relaxation of sliding blocks governed by (1) assuming $v_0 = 0$ in the friction law (2) and immobile non-sliding blocks. The slightly curved lines in Fig 2(b) are the effect of $v_0 \neq 0$. (iii) In the third step the boolean variable s_j is recalculated: A sliding block still slides and nonsliding block starts to slide for the same reason as in the first step. That is,

$$s_j^{\text{new}} = s_j^{\text{old}} \vee (x_{j-1} - 2x_j + x_{j+1} - F_S/\kappa > 0), \quad \text{for } j = 1, \dots, N, \quad (6)$$

where \vee denotes the boolean operator for inclusive or. (iv) Repeat steps (ii) and (iii) until no new block starts to slide in step (iii). Note that rule (ii) is a *nonlocal* rule because j_1 and j_2 can be arbitrary far from site j . This is in contrast to most other automata discussed in the field which have local relaxation rules.

The result of applying these relaxation rules are the following. The first sliding block is always block number one. In the next cycle block number two starts to slide. This goes on until no new block starts to slide. Thus the avalanche length L is the smallest positive value which fulfills

$$x_0 + (x_{L+1} - x_0)L/(L + 1) + x_{L+2} - 2x_{L+1} \leq F_S/\kappa. \quad (7)$$

After some straightforward calculations one finds that between two system-spanning avalanches 2^{n-m} avalanches occur. They are organized in the same binary tree as in the train model [see Fig. 2(b)]. The length and the strength of the m -th type are $L_m = 2^{m-1}$ and $S_m = (1 + 2^{2m-1})F_S/(6\kappa)$, respectively. Therefore the cellular automaton has exactly the same scaling exponents and log-periodicity as the overdamped train model.

The behavior of the automaton is very sensitive to nonuniformities in static friction F_S because the avalanches always stop when condition (7) is just fulfilled. We introduce quenched randomness in two different ways leading to two different behaviors.

In the first way random numbers F_{Sj} from a Gaussian distribution are assigned to each block. After each system-spanning avalanche the same sequence of avalanches appears. They are also organized in a hierarchical manner. The cumulative densities are still stairs (see Fig 4) but the heights and the widths of the steps are fluctuating. Averaging over many realizations of $\{F_{S1}, F_{S2}, \dots, F_{SN}\}$ leads to cumulative densities which still show log-periodic oscillations (see Fig. 4). The oscillation amplitude decreases with the noise level. The phase of the oscillation changes also but it still does not depend on N .

The automaton shows a different behavior if we assign to each block a new random number F_{Sj} after a slide. Figure 5 shows that the oscillations in the cumulative density vanish completely even for infinitesimally small noise level [8]. Otherwise the scaling exponents are the same as for the nonrandom case. In the underdamped case the train model is less sensitive to this kind of quenched randomness. In simulations of (1) with $\Delta F_S/\langle F_S \rangle = 10^{-2}$ we still find oscillations but with smaller amplitudes.

Why have these log-periodicities not be found for purely velocity-weakening friction laws [3]? The main reason may be that for such laws *any* sliding motion of the chain or a part of the chain is *unstable*. For a velocity-strengthening friction force, sound waves with wavelength larger than $\bar{L} \equiv 4\pi\sqrt{\kappa M}/\gamma$ are overdamped because their frequency becomes less than $\gamma/2M$. Thus

avalanches involving more than \tilde{L} blocks show regular behavior after some possibly chaotic transients. This regular behavior is very well described by the nonlocal cellular automaton. In the overdamped case (i.e., $\tilde{L} \lesssim 1$) the regular motion successively amplifies the smallest intrinsic length scale (i.e., $L = 1$) by the factor two. This basic mechanism is responsible for discrete scale invariance which would be destroyed by the intrinsic instabilities cause by a velocity-weakening friction force. It is unclear, why in the underdamped case (i.e., $\tilde{L} \gg 1$) discrete scale invariance also occur. The mechanism has to be a different one because the motion of a group of less than \tilde{L} blocks is in general irregular. Two observations may help to explain this phenomenon: (i) The steps in the cumulative density of L do not occur at powers of two but at $aN/\tilde{\lambda}_L^n$, for $n = 0, \dots, \tilde{n}$, where $\tilde{\lambda}_L \approx 2$, a is an N -independent number between 1/2 and 1, and \tilde{n} is clearly less than $\ln(aN/\tilde{L})/\ln 2$. (ii) Although the large avalanches are organized in a binary tree, their sequence of occurrence is different. Let us consider a big avalanche much bigger than \tilde{L} but not a system-spanning one. Looking for a considerably bigger avalanche in the past and in the future we find that in the overdamped case both time intervals are the same whereas in the underdamped case the time interval in the past is much smaller than the time interval in the future. In fact only a handful of very tiny avalanches occur in the time interval in the past.

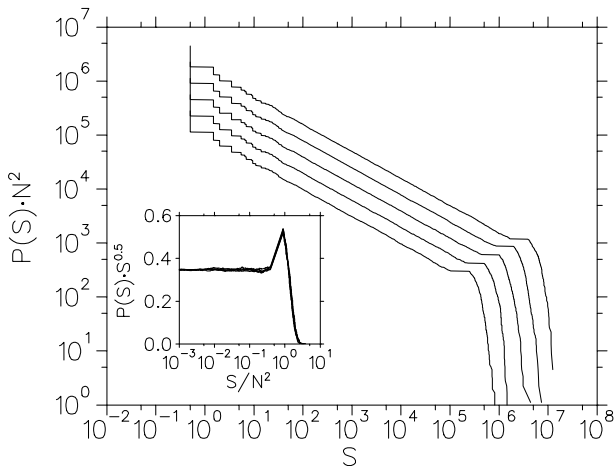


FIG. 5. The cumulative density $P(S)$ of the cellular automaton with randomly chosen static friction F_S which changes after each slide. The parameters are $\langle F_S \rangle = \kappa = 1$, $\Delta F_c = 10^{-3}$, and $N = 530, 750, 1060, 1500$, and 2121 . The cumulative densities are shifted by $2 \log N$ in order to separate them. The inset show the scaling function G .

We have shown that SOC with complex scaling exponents occurs in the train model with a *realistic* velocity-strengthening friction law. We are confident that other depinning models may also show discrete scale invariance. The key ingredients are the following: (i) There

should be a bistability between pinning and sliding for the same local force. This can be either achieved by inertia of the pinned objects or by age-dependent pinning (i.e., the pinning force which increases with the pinning time). (ii) The sliding dynamics should be nonchaotic with diffusion-like relaxation of long-wavelength excitations. In BK-like models a velocity-strengthening friction laws are a necessary condition for that. (iii) Quenched randomness in the pinning forces should be absent or weak. The first two properties are necessary to get non-local deterministic relaxations rules similar to our automaton. These rules are responsible for discrete scale invariance because they either amplify successively an intrinsic (microscopic) length scale up to the system size by a constant factor or vice versa. Quenched randomness distort these process leading to fluctuations of the phase of the log-periodicity which may be smeared out if they are too strong.

ACKNOWLEDGMENTS

I gratefully acknowledge D. Sornette who introduced me into the concept of discrete scale invariance, H. Thomas for critical reading of the manuscript, and the Centro Svizzero di Calcolo Scientifico at Manno, Switzerland, for doing the simulations on the NEC SX-3 and SX-4.

-
- [1] P. Bak, C. Tang, and K. Wiesenfeld, Phys. Rev. Lett. **59**, 381 (1987).
 - [2] for a review see e.g. D. Sornette, Phys. Rep. in press (1997).
 - [3] M. de Sousa Vieira, Phys. Rev. A **46**, 6288 (1992).
 - [4] R. Burridge and L. Knopoff, Bull. Seismol. Soc. Am. **57**, 341 (1967).
 - [5] A more realistic friction law would be velocity-weakening for small velocities and velocity-strengthening for large velocities. Such laws are used in Ref. [4]; V.G. Benza, F. Nori, and O. Pla, Phys. Rev. E **48**, 4095 (1993); J.H.E. Cartwright, E. Hernández-García, and O. Piro, Phys. Rev. Lett. **79**, 527 (1997); F.J. Elmer, J. Phys. A **30**, 6057 (1997).
 - [6] There is no clear distinction between underdamped and overdamped motion because it depends on the wave length of the sound waves. For $\gamma < \sqrt{\kappa M \pi}/N$ all sound waves are underdamped and for $\gamma > 4\sqrt{\kappa M}$ all sound waves are overdamped.
 - [7] The right most step occurs at $L = N$ which does not fits into this power-of-two scheme.
 - [8] That is, for $\Delta F_S / \langle F_S \rangle$ approximately below (above) ϵ the cumulative densities do (not) oscillate.